

## Climatic Fields of Horizontal Temperature Gradients of Water in the South Atlantic

L. I. Galerkin, A. M. Gritsenko, and S. G. Panfilova

Presented by Academician M.E. Vinogradov August 8, 2005

Received August 10, 2005

DOI: 10.1134/S1028334X06040222

The vertical structure of ocean water has been sufficiently well studied at present. Its principal elements—layers of discontinuity, warm and cold layers, saline and fresh layers, and their statistic and extreme characteristics—are known at all spatial and temporal scales. The horizontal structure of hydrophysical fields in oceans is less understood. Investigations were mainly restricted to the compilation of maps of temperature, salinity, density, and calculated currents.

Positions of fronts, temperature gradients, salinity, and their extrema were assessed visually based on the density of contours. Quantitative assessments of the horizontal structural elements were carried out very rarely. Fronts and frontal zones were mainly studied in the Gulf Stream and Kuroshio regions. Studies in other oceanic regions have been scanty. Some detailed hydrogeological surveys and test sites have yielded good assessments, but they are restricted to very limited time intervals and water areas. Owing to the random and nonsystematic nature of such field measurements, one cannot make quantitative assessments on a scale of months and years and obtain generalized conclusions for large ocean areas.

This work presents new results from calculations of one of the most important structural elements—horizontal gradients of the temperature field based on average climatic data—discussed in [1, 2]. The calculations were based on annual mean monthly data in one-degree spherical IDC-A trapeziums in the United States for the South Atlantic sector extending from the equator to Antarctica [3]. Hydrophysical fields averaged in the selected area provide reliable calculations and climatically significant results.

Increase in horizontal gradients is known to be an indicator of hydrological fronts and frontal zones separating water masses or circulation systems. The long-term preservation of relatively high values of horizontal

gradients is an essential property of climatically stable frontal boundaries, although they usually tend to become vague due to turbulence, synoptic vortices, and other disturbances of the quasi-stationary field. This fact is a strong argument for studying fronts and frontal zones based on climatic data.

Horizontal gradients ( $G$ ) were calculated by the numerical differentiation method based on five adjacent temperature ( $T$ ) values along the meridian and parallel. Then, the module and the  $G$  vector direction were determined based on their components. At a degree equal grid of the field, the linear distance between points along the meridian remains constant. Along the parallel, the distance is calculated with an allowance for the cosine latitude. The dimension of the  $G$  module is °C per 60 miles (111 km).

The analysis of study coverage maps for each month shows only one to three observations in one-degree squares in the southern water area extending from 30°–35° S to Antarctica. More than one-half of the squares in the central South Atlantic have not been investigated at all. The number of observations increases in narrow coastal zones along Africa and South America, as well as around the Falkland Islands, South Georgia Island, and South Orkney Islands.

The general configuration of  $G$  contours on both maps (Fig. 1) shows their predominant latitudinal orientation related to general water circulation. Alternation of areas of relatively high and low  $G$  values is prominent. Symbols on the maps designate axial lines of high  $G$  values associated with frontal zones. For brevity sake, we shall refer to them as fronts.

The subtropical front in the summer (February) map begins near the American coast and extends between 40° and 45° S up to 25° W. Then it shifts northward up to 32° S and ends at the Greenwich meridian. The maximum  $G$  values are 1.5–1.7 in the western and central parts of the ocean and 0.6–0.8 in the eastern part. In the winter (August) map, the subtropical front in the central part of the ocean is located at 33°–36° S. The eastern branch runs between 40°–43° S to the ocean bound-

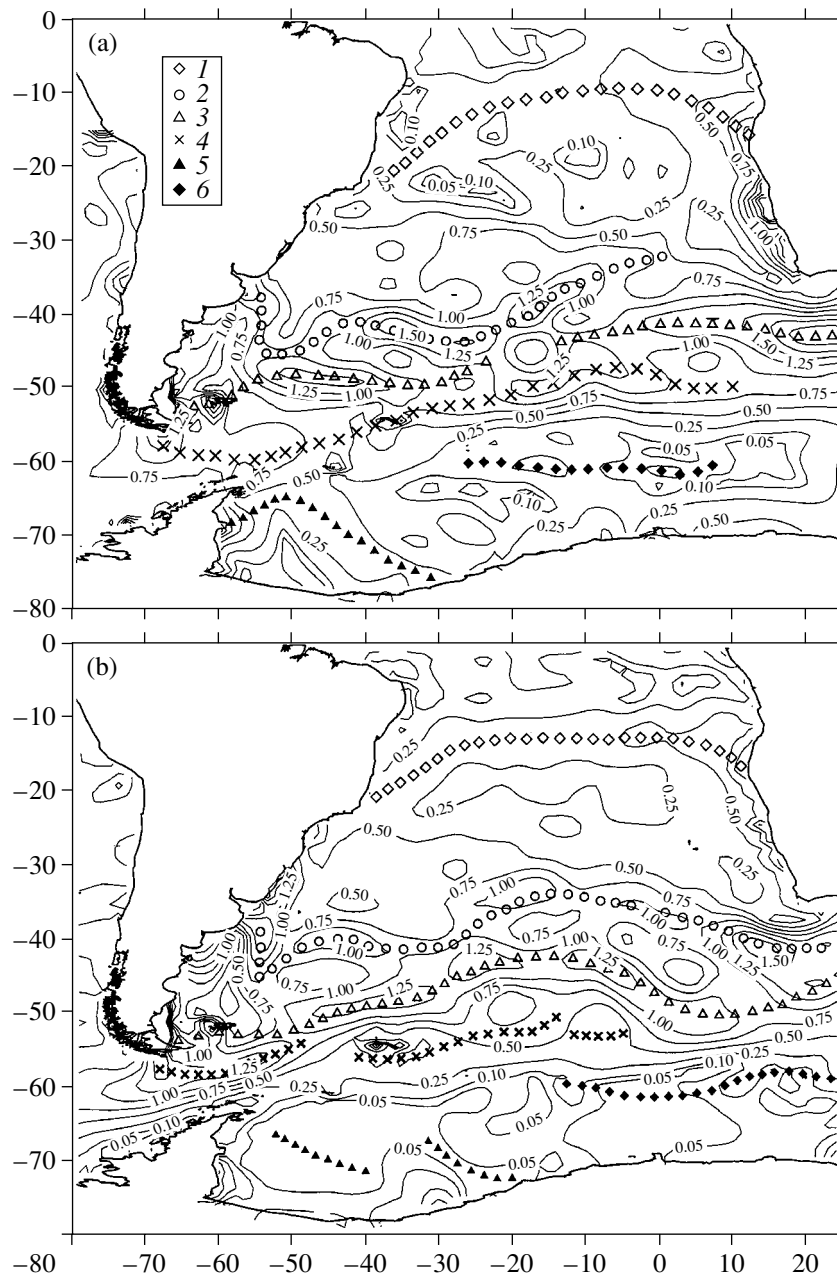


**Fig. 1.** Water temperature gradient on the South Atlantic surface: (a) in February; (b) in August. (1) Tropical frontal zone; (2) subtropical frontal zone; (3) subantarctic frontal zone; (4) polar frontal zone; (5) Weddell Sea front; (6) Antarctic front.

ary.  $G$  values throughout the whole front in the western and central parts of the ocean are lower (1.2–1.5) than in summer and equal to 1.8–1.9 in the eastern part.

Both maps show a sharp southward bend of the subtropical front along  $55^\circ$  W with a subsequent northeastward turn caused by a merger of cold waters from the Falkland Current with warm waters from the Brazil Current and their simultaneous southward and southeastward turn [4, 5].

In the winter and summer, the subantarctic front extends through the whole ocean. In the western part, it is located  $3^\circ$ – $5^\circ$  farther southward in the winter relative

to in the summer. In the central part ( $15^\circ$ – $25^\circ$  W), the front is split into a vast low-gradient area in August. This is most likely related to a small number of observations and an unsuccessful method of initial data interpolation rather than a natural phenomenon. Breaks in fronts and frontal zones may be related to random (in space and time) observations of different-scale heterogeneities, which substantially distort the climatic field if the measurements are insufficient. East of  $10^\circ$  W, the latitudinal position of the subantarctic front in the winter is located  $5^\circ$ – $10^\circ$  farther southward than in the summer. In the western and central parts,  $G$  values in the

Parameters of the annual trend of the average temperature gradient in the 0–200-m layer

Parameter		0	30 m	50 m	75 m	100 m	150 m	200 m	$\bar{G}_{\max}$
Max	month	Mar.	Mar.	Mar.	Apr.	Apr.	Sept.	May	May
	$G$	0.751	0.748	0.735	0.696	0.685	0.646	0.589	0.700
Min	month	Sept.	Aug.	Aug.	Sept.	Nov.	Feb.	Aug.	Sept.
	$G$	0.626	0.622	0.621	0.617	0.635	0.610	0.558	0.646
$G_{\max}-G_{\min}$		0.125	0.126	0.114	0.079	0.050	0.036	0.031	0.054
Annual $\bar{G}$		0.694	0.687	0.678	0.659	0.657	0.625	0.574	0.669
Maximum growth rate		Sept.–Oct.	Sept.–Oct.	Sept.–Oct.	Sept.–Oct.	Sept.–Oct.	Aug.–Sept.	Aug.–Sept.	Sept.–Oct.
		0.050	0.046	0.029	0.030	0.013	0.026	0.033	0.029
Maximum fall rate		Apr.–May	Apr.–May	Apr.–May	June–July	July–Aug.	Oct.–Nov.	July–Aug.	Apr.–May
		0.046	0.036	0.025	0.033	0.049	0.017	0.013	0.041

winter are 0.2–0.4 units lower than in summer. The values are equally higher in the eastern part.

The polar front extends south of the subantarctic front. It begins in both seasons in the Drake Strait. In summer, it runs southeastward to the South Shetland Islands and turns northeastward, gradually departing northward up to 47°–48° N and terminating at 10° E. In the Drake Strait and on the eastern side, the polar front shifts in the winter to 55°–57° S (i.e., farther northward than in summer). In the central part, the front is located 5°–10° southward. In August, this front consists of three parts and ends at 3°–5° W. Maximum gradients near Cape Horn in the winter make up 1.7, decreasing in summer to 1.5. In the eastern part,  $G$  values decrease in the winter to 0.6–0.4. In the central part (25° W–0°), the gradient increases to 1.0–1.4 in the summer.

The eastern and central parts accommodate one additional front, the position of which changes by 2°–3° relative to 60° S. In the winter, this front abruptly terminates near 15° W and continues in the summer to 30° W.  $G$  values vary along the front from 0.03 to 0.15 in the winter and reach 0.3 in the summer. Links of this front with climatic or circulation processes are as of yet unknown. Probably, the “Antarctic” front separates some streams of the Circumpolar Current and restricts water circulation in the Weddell Sea in the north [5].

The frontal zone of the Weddell Sea is the southernmost one. It exists as a single front only in the summer and is split into two different (in length and orientation) fragments in the winter. In the western part,  $G$  values are up to 0.5 in the summer and up to 0.1–0.2 in the winter.

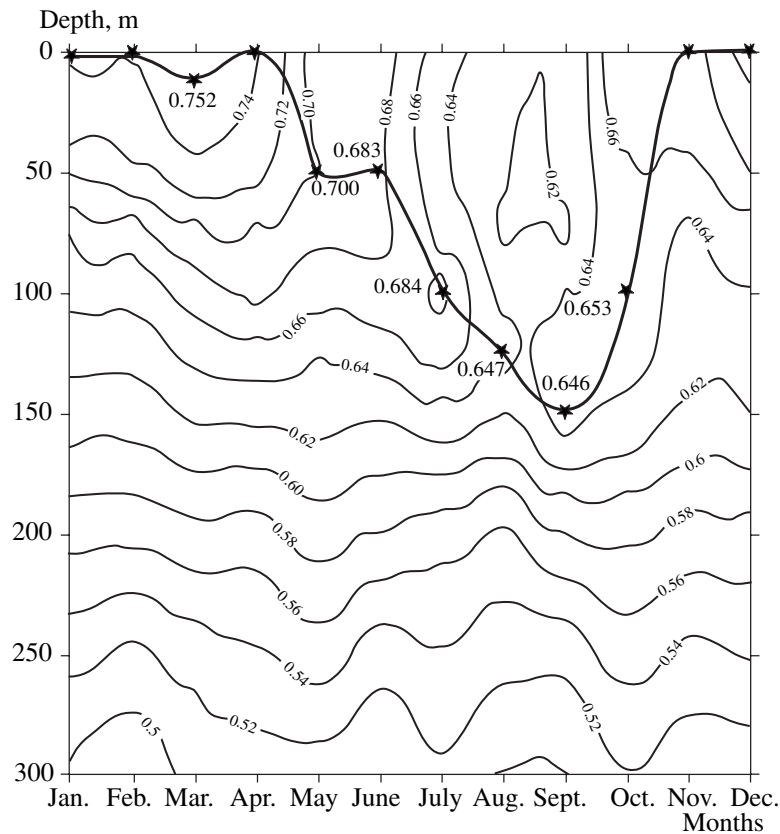
In the South Atlantic, maximum temperature gradients are characteristic of a small bay north of the entrance to the Strait of Magellan. The highest values (4.83 and 4.79) are recorded in transitional seasons (April and October), whereas the lowest values (4.16 and 3.95) are typical for February and July.

We have calculated the climatic statistics for the field of horizontal temperature gradients of water in the Atlantic sector of the South Ocean. Statistics of the  $G$  value were calculated for horizontal fields at 19 levels from 0 to 1000 m for each month. We present here the analysis of the first moment of distribution (the average  $\bar{G}$  value for the whole water area south of 35° S).

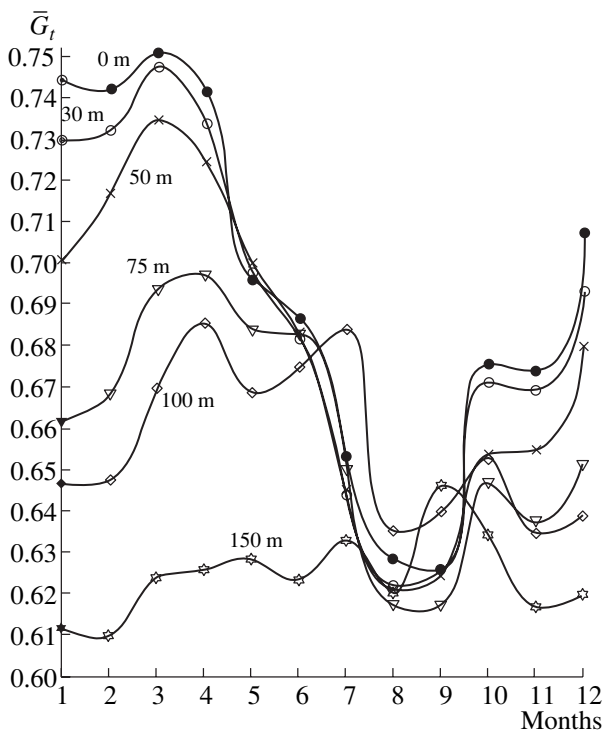
Figure 2 illustrates  $\bar{G}$  isopleths (in terms of time and depth) in the 0–300 m layer. Vertical profiles in the 0–1000 m layer show the existence of only one  $\bar{G}$  maximum on the surface in the 0–75 m layer in the warm season (November–April). A second maximum appears at 50 m in May and reaches a depth of 150 m in September and 100 m in October. The maximum disappears in November. The last column of the table shows basic characteristics of the subsurface extremum. One can see a monotonous decrease in gradients at 200–1000 m in all the twelve-month profiles. At the depth of 1000 m, the highest  $\bar{G}$  value (0.153) is recorded in December, whereas the lowest value (0.137) is typical for August.

Figure 3 demonstrates the annual  $\bar{G}$  trend in the upper (0–200 m) layer. The layer shows a monotonous decrease in the annual trend. The analysis of  $\bar{G}$  variations at different levels during a year shows only one maximum at 0–75 m. The maximum is steady at 0–50 m in March, at 75–125 m in April, and at 150–1000 m in May. A second maximum appears at 100 m in July. The maximum shifts to 400 m by December and extends to a depth of 1000 m in this month. The second (winter–spring) maximum is 0.1–0.05 units lower than the autumn (March–June) maximum.

Phases of the annual trend coincide almost at all the levels. The decrease in maximum  $G$  values at 0–200 m is rather high (from 0.751 to 0.589). In the minimal months (August and September), horizontal scatter in



**Fig. 2.** Isopleths of the annual trend of the average temperature gradient with depth. Asterisk designates the line connecting maximum gradients at each depth level.



**Fig. 3.** Annual trend of temperature gradient in 0–150-m layer in the South Atlantic south of 35° S.

temperature gradients along the horizontal extent at 0–150 m is almost ten times lower (0.162 at the end of summer and 0.017 in winter). The presence of a distinct second maximum indicates that seasonal variations in the whole water area of the study region include a clearly defined semiannual wave in intermediate layers down to a depth of 1000 m.

The table demonstrates basic parameters of the annual  $\bar{G}$  trend at seven levels. For the quantitative assessment of the annual  $G$  variation, we calculated not only the annual trend range ( $\bar{G}_{\max} - \bar{G}_{\min}$ ), but also the extreme growth and fall rates of  $\bar{G}$  values (see the last rows of the table. At 0–100 m, the maximum growth rate remains steady at the end of winter (September and October). At 150 and 200 m, the maximum begins a month earlier (August and September). The  $\bar{G}$  growth rate is four times lower in the upper layer (0–100 m) and increases again at 100 and 200 m. In the upper layer (0–50 m), the maximal decrease rate is recorded in April and May. At 75–150 m, the maximum decrease is recorded in June–July and October–November. This trend is observed in July–August at 200 m. The decrease rate shows a wavy character: a decrease at 0–50 m, an increase at 50–100 m, and a decrease again at

100–200 m. The last column of the table presents the same characteristics of  $\bar{G}$  positions and values in terms of depth.

Thus, we have found a regular dependence and succession of climatic frontal zones even after a small number of observations. In winter months, the maximum value of the average gradient in the water area is observed in the lower part of the upper subsurface layer, and gradient values are minimal at all the levels. Extremely high gradients become subordinate in the winter and descend from the surface to a depth of 150 m. Scatter in values between layers in the whole subsurface layer does not exceed 0.014.

## REFERENCES

1. L. I. Galerkin, A. M. Gritsenko, S. G. Panfilova, and A. D. Yampol'skii, Dokl. Akad. Nauk **384**, 539 (2002) [Dokl. Earth Sci. **384**, 473 (2002)].
2. L. I. Galerkin, A. M. Gritsenko, S. G. Panfilova, and A. D. Yampol'skii, in *International Conference "Expedition Investigations of the World Ocean and Informational Oceanographic Resources (OIR-98)" Abstracts of Papers* (VNIIGMI-IDC, Obninsk, 1998) [in Russian].
3. S. Levitus and T. P. Boyer, *World Ocean Atlas* (NOAA, Washington, 1994), Vol. 4.
4. R. G. Peterson and T. Whitworth III, *J. Geophys. Res.* **94**, 10817 (1989).
5. L. Stramma and R. G. Peterson, *J. Phys. Oceanogr.*, No. 20, 846 (1989).